Microgravity Mapping of an Inception Doline Shaft System

PETER J. HUTCHINSON*
ALEXANDER BALOG

THG Geophysics, Ltd., 4280 Old William Penn Highway, Murrysville, PA 15668

SHAD E. HOOVER

CMT Laboratories, Inc., 2701 Carolean Industrial Drive, State College, PA 16801

Key Terms*: Sinkhole, Doline, Subsidence, Grout Stabilization*

ABSTRACT

Reactivation of an inception doline shaft system through anthropogenic actions, precipitation, and possibly seismic activity induced subsidence in a hospital emergency room that was under construction in State College, PA. The convergence of Tropical Storm Lee and Hurricane Irene is interpreted to have caused the building's brick edifice to fall and induce vertical shifts in the reinforced concrete entrance floor slab. Microgravity mapping of the existing hospital emergency room entrance; the emergency room building under construction; and the parking lot in front of the emergency room entrance documented the presence of a doline shaft system (i.e., inter-connected sinkhole). Groundwork for the construction of the new emergency room included grading and leveling of the property. Surface water runoff entered the construction site from a parking lot that sloped toward the addition and to a non-functioning stormwater inlet. The grading for the new construction exposed an open fracture for surface runoff. Subsequent channeling of surface water to the conduit provided drainage for surface runoff, but it also initiated subsidence throughout the existing structure and the addition that was under construction. Engineering rehabilitation included a limited mobility (LM) grout program to plug subsoil fracture karren drainage systems and stabilize the surface. Drilling progressed in four stages, initially focusing on areas of greatest subsidence. In total, 60 injection points were completed to a mean depth of 24 m below grade in an area measuring approximately 370 m^2. During LM grouting, 867 m^3 of a sand-and-cement grout mixture were injected to stabilize the area.

*Corresponding author email: pjh@thggeophysics.com

INTRODUCTION

In March of 2011, Mount Nittany Medical Center (MNMC) started construction of an emergency room adjacent to the existing emergency room (Figure 1). By April, the grading and filling had been completed, and foundation excavations for the new addition commenced.

Between August 28 and 29, 2011, Hurricane Irene dumped 1.7 cm of rain on the project site. Subsequently, Tropical Storm Lee dumped an additional 13.7 cm of rain from September 5 through 9, 2011 (Figure 2).

On or before September 7, 2011, portions of the front façade collapsed, and the floor to the existing emergency room showed structural damage. On September 13, subsidence to the support columns for the new emergency room was also noted (Figure 1).

Discussions with the construction crew revealed that during site-grading activities, an opening was discovered in the subsurface between the two buildings (Figure 3). Surface water was then channelized to the narrow opening by the construction crew to help clear the site of ponded water. The opening was probably an extension of a fracture/void from a subsurface karren (i.e., a rugose type of rock texture) in the underlying bedrock that had been exposed by the grading activities.

GEOLOGY

MNMC is located within Nittany Valley, in the northwestern margin of the Valley-and-Ridge Province (Fenneman, 1938; Faill and Nickelsen, 1999; Faill, 2000; and Miles and Whitfield, 2001). The Valley-and-Ridge Province is the western-most portion of the Alleghenian foreland fold-and-thrust tectonic belt (Nickelsen, 1988; Figure 4). The foreland fold-and-thrust belt is characterized by décollement-based deformation as part of the Allegheny Orogeny (Boyer and Elliott, 1982; Geiser and Engelder, 1983). In this style of deformation, an allochthonous mass of

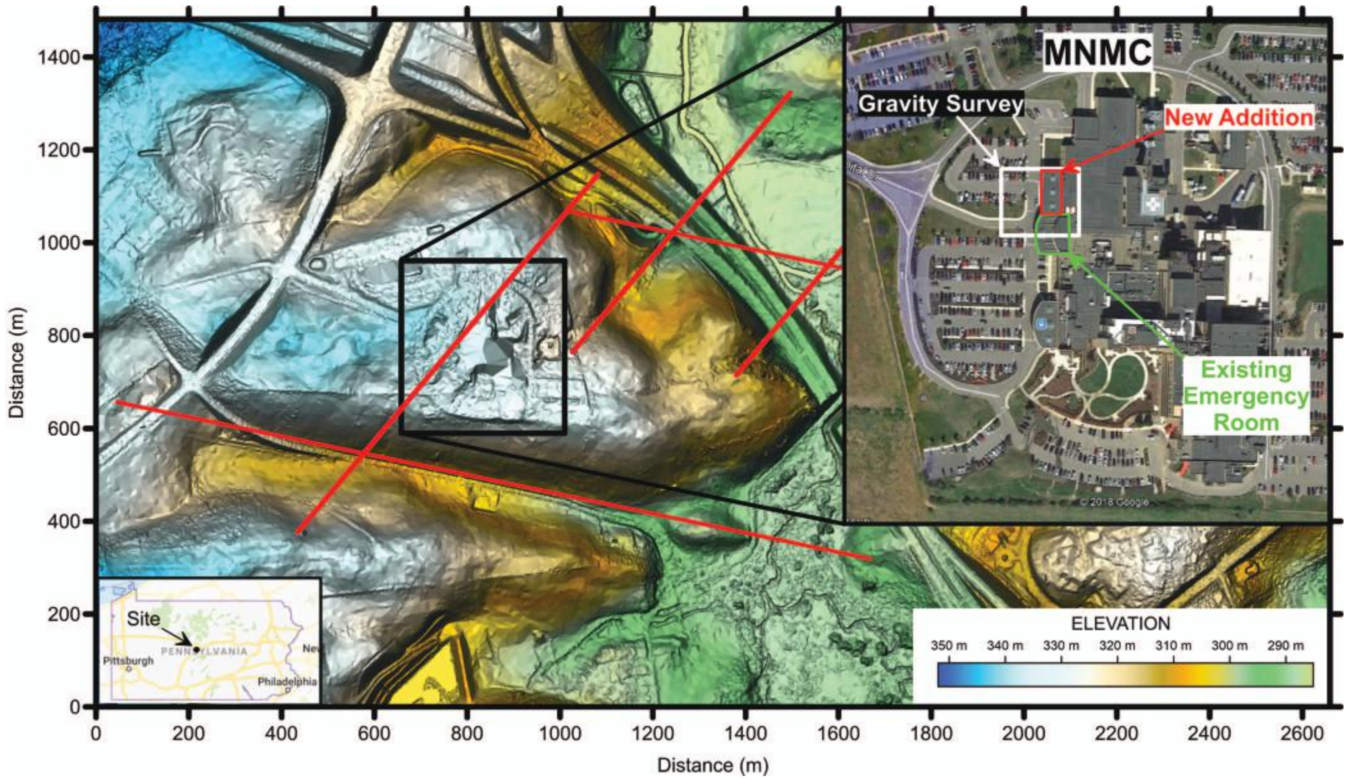

Figure 1. Digital elevation model (1 m grid; North American Vertical Datum of 1988; 2006–2008 Department of Conservation and Natural Resources PAMAP) showing inferred fractures in red. Inset is from Google Earth (2018) showing the footprint of the gravity study area (white), new hospital addition (red), and existing emergency room (green).

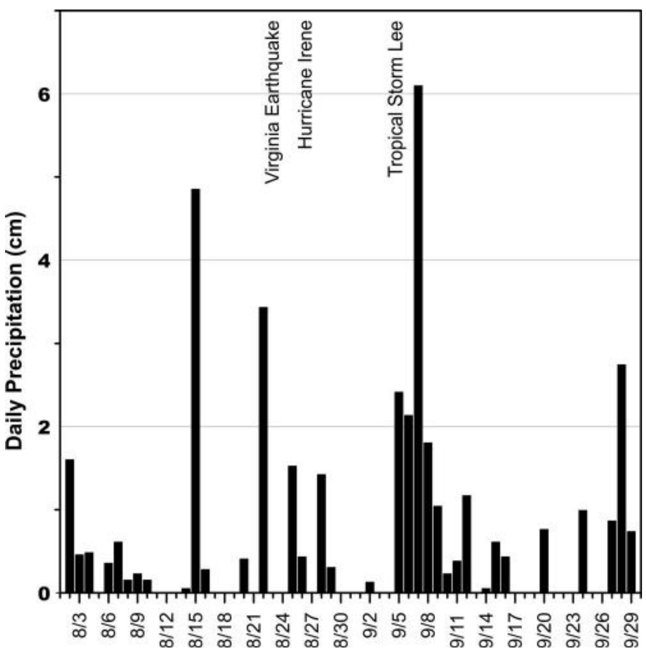

Figure 2. Daily precipitation for State College, PA, August through September 2011.

foreland rocks moves as a thrust sheet on a subhorizontal fault (décollement) outward from an orogenic core towards the craton (Chapple, 1978; Faill, 1997a, 1997b, 1998).

At a depth of about 7 km below grade, the basal décollement consists of the Cambrian Potsdam Formation detaching from the Cambrian Tomstown Formation (Figure 5). The shallowest décollement is the top of the Ordovician Reedsville Formation with the base of the Cambrian Potsdam Formation (Berg et al., 1980). This thrust sheet brought the Nittany Dolomite to the surface as a gentle fault-bend fold anticline (Figure 5). Due to stacking of the carbonate suites on two décollements, there is an estimated 7,000 m section of carbonate rock beneath the MNMC (Demicco and Mitchell, 1982; Gold et al., 2017). The formation of fault-bend fold anticlines further deformed the carbonates by creating a stress environment conducive to carbonate dissolution and fracturing.

Within the footprint of the MNMC, periglacial clay-rich silt and sand unconformably overlie the Lower Ordovician Nittany Dolomite (Parizek et al., 1971). The Nittany Dolomite is a medium- to dark-gray, thick-bedded dolomite containing chert and siliceous

Figure 3. Fracture discovered during grading operations. Note the iron staining on the wall of the fracture.

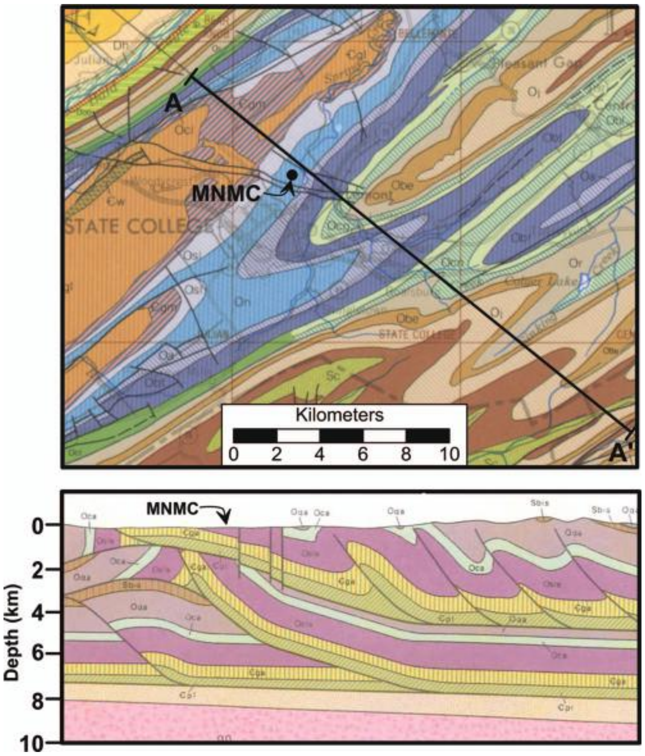

Figure 4. Geologic map and section (Berg et al., 1980). Note geologic colors and descriptions differ between the two images. No vertical exaggeration to the profile. Map key: Precambrian granitic gneiss (gn): Cambrian Tomstown (Ꞓl), Warrior (Ꞓw),;Gatesburg (Ꞓgm and Ꞓgl): Ordovician Stonehedge/Lark (Osls); Nittany (On); Axeman (Oa); Bellefont (Obf); Brenner (Obv); Coburn (Ocn); Reedsville (Or); Bald Eagle (Obe); Juniata (Oj): Silurian Shawangunk (Ss); Clinton Group (Sc). Profile key: Precambrian granitic gneiss (gn): Cambrian Tomstown (Ꞓwh); Potsdam (Ꞓpl); Gatesburg (Ꞓga): Ordovician Stonehedge/Lark, Nittany, Axeman, and Bellefonte (Osls); Brenner and Coburn (Oca); Reedsville (Orm); Bald Eagle (Obe); Juniata (Oj); Queenston (Oqa): Silurian Shawangunk and Clinton Group (Sbis).

oolites with an estimated thickness in this area of 360 m. The Nittany Dolomite is characterized by having large-scale drawdown dolines (for example, State College's Memorial Stadium is a partially exhumed doline).

The Nittany Dolomite conformably overlies the Stonehenge Limestone, which is aphanitic to fine grained, argillaceous and dolomitic in part, and contains abundant flat pebble conglomerate lenses. The Ordovician Stonehenge Limestone is approximately 180 m thick and is only locally karst forming.

Conformably underlying the Lower Ordovician Stonehenge Limestone are the Upper Cambrian Gatesburg and Warrior Formations. Both formations are karst-forming dolomites with a total thickness of 850 m.

Karst Evolution

Deeply buried limestones can undergo metasomatic processes (dolomitization) that rearrange and enlarge pores (Wilson, 1975; Sibley, 1982; and Hem, 1989). During the formation of dolomite, the net rock volume of limestone decreases by 13 percent, leaving voids and vugs that can induce further dissolution through increased permeability (Hohlt, 1948).

$$2CaCO_3 + Mg^{2+} \leftrightarrow CaMg(CO_3)_2 + Ca^{2+}. \quad (1)$$

One important aspect of converting limestone to dolomite is that the increase in porosity and permeability within the rock creates excellent reservoirs for oil and gas production (Levorsen, 1967; Longman, 1982).

Current theories show that karst forms through two mechanisms, hypogene and epigene speleogenesis (Klimchouk, 2018). Klimchouk (2007, 2014) documented hypogene speleogenesis, or vertically upward migration of groundwater during the course of depositional history, as a mechanism for the creation of karst topography. Remanent magnetization of ferromagnesium minerals during Pennsylvanian–Permian deformation has been attributed to the vertically upward percolation of orogenic fluids through the carbonate units within the Arbuckle Mountains (Nick

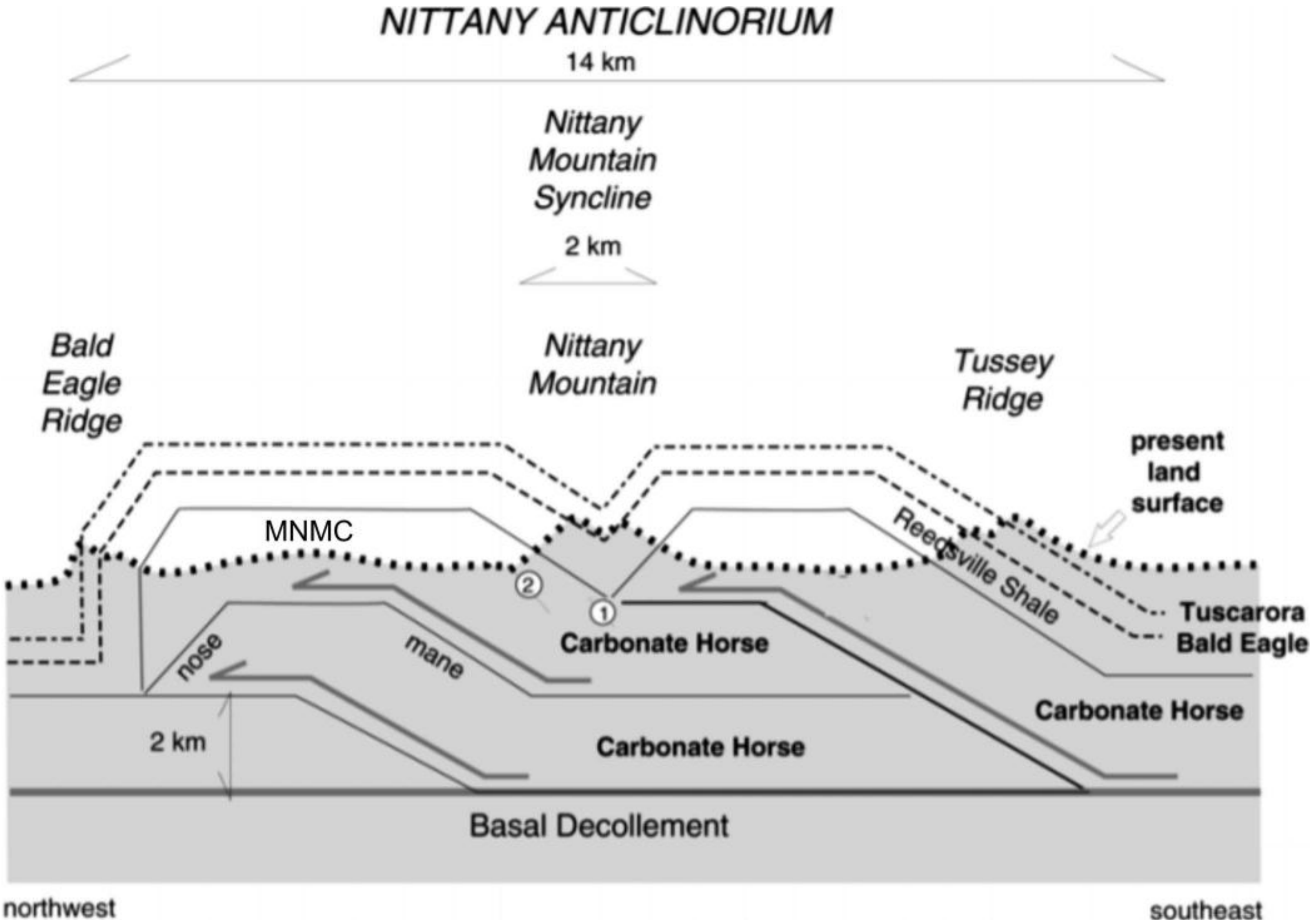

Figure 5. Profile through Nittany Mountain with indeterminate location of the upper décollement (1) and location where it is theoretically exposed (2) at the surface (from Gold et al., 2017). MNMC is the Mount Nittany Medical Center.

and Elmore, 1990) and Valley-and-Ridge Province of central Pennsylvania (Mathur et al., 2008).

Two types of karst systems are recognized in the world today: epigenic and hypogenic (Klimchouk, 2007). Regional groundwater flow systems provide the systematic transport and distribution mechanisms needed to produce and maintain the disequilibrium conditions necessary for speleogenesis. Epigenic karst systems exist in unconfined groundwater conditions and are predominantly local systems, whereas hypogenic karst is associated with discharge regimes of regional flow systems. Hypogenic speleogenesis occurs within confined groundwater settings and may lose the confining groundwater conditions due to uplift. The confined cave systems can be further modified under unconfined groundwater conditions through epigenic processes.

The primary criteria for identifying hypogenic caves are morphological and hydrogeological features. Hypogenic caves have network mazes, spongework mazes, irregular chambers, and isolated passages or crude passage clusters. They often combine to form composite patterns and complex three-dimensional structures.

Hypogenic caves have an areal coverage that is five times greater than in epigenic karst systems (Klimchouk, 2007). Hypogenic speleogenesis commonly results in more isotropic conduit permeability within highly karstified areas measuring up to several square kilometers. Hypogenic speleogenesis contributes to hydrothermal mineralization, diagenesis, and hydrocarbon transport and entrapment.

Hypogenic processes have contributed to the inception dolines within the study area. Deformation in the form of a fault-bend fold anticline increased permeability and provided more opportunity for metasomatic processes. Rauch and White (1970) noted that most caves in the Nittany Valley occur within limestone epigene karst and that cave development in dolomite is extremely rare. However, dolines are common in the Nittany Dolomite, which points to a

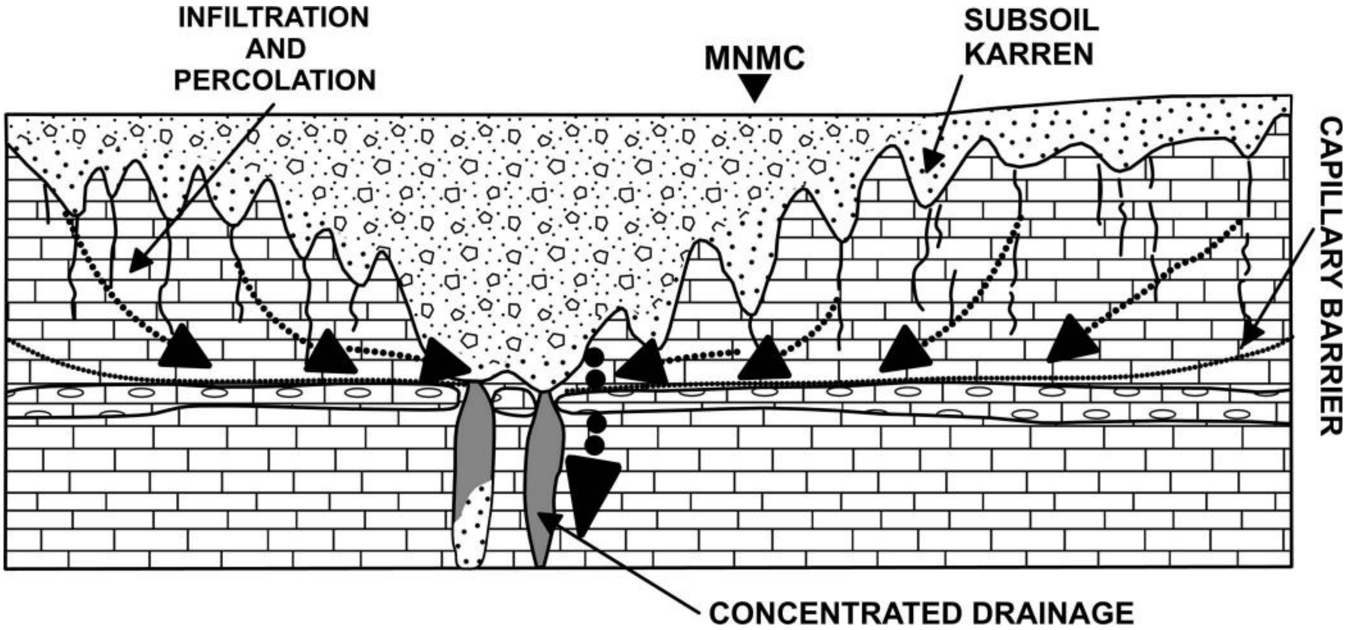

Figure 6. A profile of an inception doline filled with periglacial soil and showing karren structures (modified from Sauro, 2012). Figure is not to scale.

deep burial environment in a hypogene environment (Figure 6).

Hearn et al. (1987) noted that during the Alleghenian Orogeny, regional potassic alteration in unmineralized carbonate rocks and mineralization in carbonate and other sedimentary deposits were related to deep brines migrating towards the basin margin under a hydraulic gradient. Also, late Paleozoic orogenic fluid expulsion from the evolving Appalachian-Ouachita Orogen increased vertically upward migration of orogenic fluids (Oliver, 1986; Duane and de Wit, 1988; and Bethke and Marshak, 1990). Consequently, fluid movement of orogenic fluids through fractures and faults resulted in the development of hypogene karst.

Further, Mathur et al. (2008), in their work with fluid inclusions, noted that late Paleozoic–aged, vertically upward, low-temperature hydrothermal migration deposited sulfide minerals (i.e., epithermal pyrite) in fractures and faults (note the staining on the wall of the fracture in Figure 2). Later, during the Cenozoic, it is speculated that the Chesapeake Bay bolide or meteor impact event triggered overprinting of the late Paleozoic mineralization through vertically upward migration of high-temperature fluids (Mathur et al., 2015).

Consequently, several mechanisms can be attributed to the vertically upward migration of water during episodic mountain-building events. Consequently, the hypogenic paradigm of the movement of orogenic fluids, both low and high temperature, left deep-seated voids.

Microgravity Theory

Microgravity measurements are not readily impacted by cultural noise; consequently, microgravity measurements can be collected in buildings and adjacent to urban development (Milsom, 1989). Microgravity has been used for many geologic purposes; however, for the environmental geophysicist, microgravity is used to determine the presence of subsurface voids, to image subsurface bedrock topography, and to find the depth of waste (Carmichael and Henry, 1977; Stewart, 1980; and Kick, 1985).

Small changes in rock density produce small changes in the gravity field that can be measured by the microgravimeter (Hinze, 1990). These readings change from day to day due to tidal response and lunar pull, among other phenomena, that have an impact on Earth's gravitational flux. Processing raw gravity data includes corrections for latitude, elevation, Bouguer gravity, tidal action, and terrain.

A microgravimeter measures the acceleration due to Earth's gravitational field in meters per second squared (m/s^2) using an astatic spring mechanism (Carmichael and Henry, 1977). Earth's gravitational field is roughly equivalent to a sphere, with variations for sea level and elevation (Nettleton, 1976; Woollard, 1975; and Milsom, 1989). The 1980 International Gravity Formula (Moritz, 1980) for calculating absolute gravity is:

$$g_{\phi} = g_o\left(1 = \alpha \sin^2\phi - \beta \sin^2 2\phi\right), \quad (2)$$

where g_ϕ is the theoretical acceleration due to gravity at a given latitude, and α and β are constants that depend on the amount of flattening of the spheroid and upon the speed of rotation of Earth (Kaufman, 1992; Reynolds, 2011). Gravity is calculated in units of acceleration, and so the SI unit for the pull of gravity is meters per second squared (m/s^2).

The International Gravity Formula was refined to the Geodetic Reference System 1967 (Woollard, 1975) and was derived (Moritz, 1980) thus:

$$g_\phi(1980) - g_\phi(1967) = (0.8316 + 0.0782\sin^2\phi - .0007\sin^4\phi)\mu\text{m/s}^2. \quad (3)$$

Latitude corrections are automatically corrected in the microgravimeter by subtracting the International Gravity Formula normal datum from the observed gravity measurement:

$$G_l = \frac{8.12\sin 2L}{\text{km}}, \quad (4)$$

where G_l is the theoretical local gradient; L is the latitude; and km is kilometers.

The elevation or free-air correction normalizes the gravity data to a given datum that does not have to be sea level. Free-air correction is based upon the free-air correction of 3.0855 μm/s^2 (ASTM, 2018). The normal elevation (h) adopted for this survey was 350 m above mean sea level (amsl), and elevation changes above this were corrected as:

$$\Delta g = g(\text{R}) \times 2h/\text{R}, \quad (5)$$

where the change in gravity (Δg) based upon elevation was derived from Earth's radius ($R = 6{,}378$ km) and normal gravitational field g (9.80 m/s^2) when corrected for h.

Bouguer corrections (b) account for the rock mass between the measuring station and sea level and are based upon:

$$b = 2\pi\rho g_s h, \quad (6)$$

where Bouguer gravity is related to density (ρ = 2.54 mg/m^3) and known thickness (h) above sea level.

Microgravity Field Survey

The CG-5 microgravimeter (Scintrex, Concord, Ontario, Canada) contains automated features that significantly reduce the possibility of reading errors. To minimize drift, a drift calibration was conducted for over 24 hours. After completion of the drift calibration, field readings repeated to within a standard deviation of 0.05 μm/s^2.

The CG-5 was utilized to collect relative measurements that were compared to the gravitational attraction at a base station with an assumed absolute value

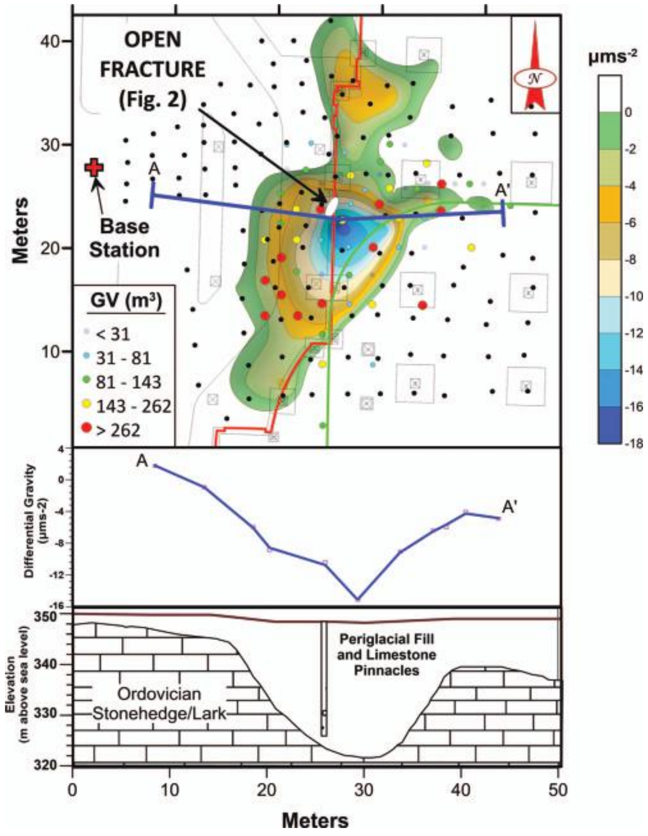

Figure 7. Differential gravity map with volumetric grout (GV) overlay. The grout injected into borings is displayed as colored dots based upon the total volume injected. Gravity measurement points are black dots; the margin of the existing emergency room building is a green line; the margin of the new emergency building is a red line; and the black squares are support columns for the two buildings. A forward modeling and inversion program, based upon the post-processed microgravity values, was used to develop the depth profile for section A-A'.

for gravity (Long and Kaufmann, 2013). A base station was established in the neighboring parking lot and re-occupied every 4 hours (Figure 7). Data points were collected on an approximately orthogonal three-meter grid pattern; however, during the field work, the survey was adjusted after the anomaly was acquired to emphasize the anomaly's dimensions.

Post-processing of all measurements is necessary prior to computing the differential gravity measurement for a particular point. The CG-5 applied an automatic gravitational tidal correction to all data based upon the diurnal variation in Earth's position to the moon and sun. Further, measurement point elevations were collected with a differential global positioning system (Trimble GEO-7XH) and post-processed for accurate (~5 cm) terrain elevation. Terrain elevation values were then applied to the background elevation of 350 m amsl for the free-air calculation.

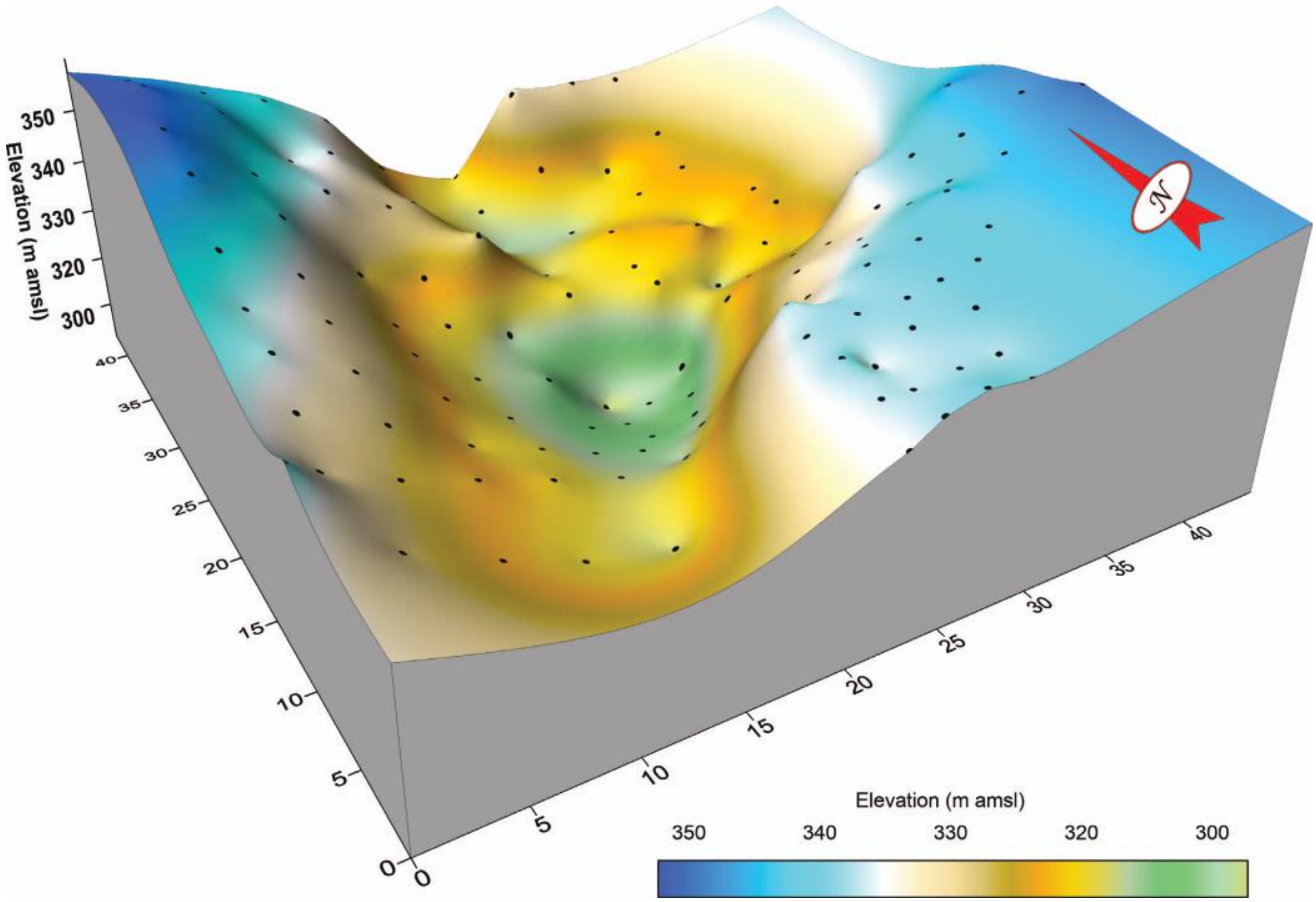

Figure 8. Pseudo–top-of-rock map based on gravity inversion modeling. Dots represent microgravity records. Note karren structures within the anomaly. All axes are in meters.

The difference between the post-processed base station and collection point value is the differential gravity for a measurement point. The differential gravity data were used to make a plan map that illustrates the difference between what is expected and what is actually measured, since the presence of voids and low-density earthen materials lowers Earth's gravitational attraction (Figure 7).

Processed gravity data were integrated into a forward modeling and inversion program (IX2D-GM; Interpex, Golden, CO) to portray a two-dimensional model of the doline (Figure 7). Unfortunately, the model does not show the open fracture in the limestone or the karren structures, but it does provide a two-dimensional conceptual model of the doline (Figure 7).

DISCUSSION

The discharge of surface runoff into the open fracture stimulated subsidence of the periglacial soil into a deep-seated fracture-based void (Figure 7). The deep-seated void evolved through dissolution from structural deformation and from vertically upward migration of cold and hot fluids, probably saline in nature. The microgravity survey identified the void as an elongate anomaly, approximately 30 m long and 10 m wide (370 m^2), which was interpreted to be a fracture-induced doline. Although the microgravity survey was too coarse to see individual pinnacles, karren features were evident in the microgravity model (Figure 8).

This fracture-induced doline is oriented north 40° east and is likely based upon deep-seated *en echelon* fractures. Surface topography supports the presence of an *en echelon* conjugate fracture system (Figure 1).

CONCLUSION

The State College, PA, area and specifically the MNMC are underlain by several thousand feet of carbonates. During construction of the new emergency room, a fracture in the subsurface was exposed. Excessive precipitation in late August and early September of 2011 was channeled to the fracture. Migration of runoff vertically downward through a fracture also mobilized the overburden in the area of the new emergency room to migrate vertically downward, creating a subsidence event for the former building and new building.

Over 100 microgravity readings were collected, processed, and compared to the processed base station reading to create a differential value. Mapping the differential microgravity readings identified the anomaly as an incipient doline. An incipient doline is generated by the convergence of water within a pre-existing structure, such as a fracture.

To correct the ongoing subsidence, borings were placed in locations thought to help prevent subsidence. LM grouting through 60 injection points, completed to a mean depth of 24 m below grade over the 370 m^2 area, stabilized the subsidence. However, since LM grouting occurred in four temporal stages, it was difficult to determine where the grout was placed three-dimensionally, since many of the injection points were connected through fractures. Ultimately, approximately 867 m^3 of a sand-and-cement grout mixture were injected into the subsurface to stabilize the area. The grouting program stabilized the surface, and thus construction continued until the building was completed. The new emergency room to the hospital is now in full use.

ACKNOWLEDGMENTS

The authors thank Heather L. Krivos, GIT, and Kate S. McKinley, PG, at THG Geophysics, Ltd., for their help with the field work. Further, we thank Whitney E. Greenawalt, PE, CMT Laboratories, Inc., for providing technical assistance after the field work was completed. We would also like to thank the three reviewers for their help: Mustafa Saribudak, David W. Abbott, and David Bieber.

REFERENCES

ASTM, 2018, *Standard Guide for Using the Gravity Method for Subsurface Investigation*, Vol. 04.09 Soil and Rock (II): ASTM International, Conshohocken, PA, 10 p.

Berg, T. M.; Edmunds, W. E.; Geyer, A. R.; Glover, A. D.; Hoskins, D. M.; Maclachlan, D. B.; Root, S. I.; Sevon, W. D.; and Socolow, A. A., compilers, 1980, *Geologic Map of Pennsylvania*, 2nd ed.: Pennsylvania Geological Survey 4th Series, Map 1, 3 sheets, scale 1:250,000.

Bethke, C. M. and Marshak, S., 1990, Brine migrations across North America—The plate tectonics of groundwater: *Annual Review of Earth and Planetary Sciences*, Vol. 18, No. 1, pp. 287–315.

Boyer, S. E. and Elliott, D., 1982, Thrust systems: *AAPG Bulletin*, Vol. 66, No. 9, pp. 1196–1230.

Carmichael, R. S. and Henry, G., 1977, Gravity exploration for groundwater and bedrock topography in glaciated areas: *Geophysics*, Vol. 42, No. 4, pp. 850–859.

Chapple, W. M., 1978, Mechanics of thin-skinned fold-and-thrust belts: *Geological Society of America Bulletin*, Vol. 89, No. 8, pp. 1189–1198.

Demicco, R. V. and Mitchell, R. W., 1982, Facies of the Great American Carbonate Bank in the Central Appalachians, *in* Lyttle, P. T. (Editor), *Central Appalachian Geology: Northeast and Southeast Sections Field Trip Guidebook*: Geological Society of America, Boulder, CO, pp. 171–266.

Duane, M. J. and de Wit, M. J., 1988, Pb-Zn ore deposits of the northern Caledonides: Products of continental-scale fluid mixing and tectonic expulsion during continental collision: *Geology*, Vol. 16, No. 11, pp. 999–1002.

Faill, R. T., 1997a, A geologic history of the north-central Appalachians; Part 1, Orogenesis from the Mesoproterozoic through the Taconic Orogeny: *American Journal of Science*, Vol. 297, No. 6, pp. 551–619.

Faill, R. T., 1997b, A geologic history of the north-central Appalachians; Part 2, The Appalachian Basin from the Silurian through the Carboniferous: *American Journal of Science*, Vol. 297, No. 7, pp. 729–761.

Faill, R. T., 1998, A geologic history of the north-central Appalachians; Part 3, The Alleghany Orogeny: *American Journal of Science*, Vol. 298, No. 2, pp. 131–179.

Faill, R. T., 2000, *Reverse Sequence of Alleghany Fold-and-Thrust Tectonics, North-Central Appalachians*: Pennsylvania Geological Survey 4th Series, 34 p.

Faill, R. T. and Nickelsen, R. P., 1999, Chapter 19: Appalachian Mountain section of the Ridge and Valley Province, *in* Shultz, C. H. (Editor), *The Geology of Pennsylvania*: Pennsylvania Geological Survey, Murrysville, PA, p. 888.

Fenneman, N. M., 1938, *Physiography of Eastern United States*: McGraw-Hill, New York, NY.

Geiser, P. and Engelder, T., 1983, The distribution of layer parallel shortening fabrics in the Appalachian foreland of New York and Pennsylvania: Evidence for two non-coaxial phases of the Alleghanian Orogeny. In Hatcher, R. D. (Editor), *Contributions to the Tectonics and Geophysics of Mountain Chains*: Memoir 158, Geological Society of America, Boulder, CO, pp. 161–176.

Gold, D. P.; Miller, C. E., Jr.; and Engelder, T., 2017, Small-scale fault-bend fold in the Appalachian Valley and Ridge Ordovician—Salona to Linden Hall section. In Anthony, R. (Editor), *Recent Geologic Studies and Initiatives in Central Pennsylvania*; 82nd Annual Field Conference of Pennsylvania Geologists, October 5–7, 2017; State College, PA, pp. 41–46.

Hearn, P. P.; Sutter, J. F.; and Belkin, H. E., 1987, Evidence for late-Paleozoic brine migration in Cambrian carbonate rocks of the central and southern Appalachians: Implications for Mississippi Valley–type sulfide mineralization: *Geochimica et Cosmochimica Acta*, Vol. 51, No. 5, pp. 1323–1334.

Hem, J. D., 1989, *Study and Interpretation of the Chemical Characteristics of Natural Water*: U.S. Geological Survey Water-Supply Paper 2254, 263 p.

Hinze, W. J., 1990, 4. The role of gravity and magnetic methods in engineering and environmental studies. In Ward, S. H. (Editor), *Geotechnical and Environmental Geophysics*: Society of Exploration Geophysicists, Tulsa, OK, pp. 75–126.

Hohlt, R. B., 1948, The nature and origin of limestone porosity: *Quarterly Colorado School of Mines*, Vol. 43, No. 4, p. 51.

Kaufman, A. A., 1992, *Geophysical Field Theory and Method: Part A, Gravitational, Electric, and Magnetic Fields*: Academic Press, San Diego, CA, 581 p.

Kick, J. F., 1985, Depth to bedrock using gravimetry: *The Leading Edge*, Vol. 4, No. 4, pp. 38–42.

Klimchouk, A. B., 2007, *Hypogene Speleogenesis: Hydrogeological and Morphogenetic Perspective*: Special Paper 1, National Cave and Karst Research Institute, Carlsbad, NM, 106 p.

Klimchouk, A. B., 2014, The methodological strength of the hydrogeological approach to distinguishing hypogene speleogenesis. In Klimchouk, A. B.; Sasowsky, I.; Mylroie, J.; Engle, S. A.; and Engle, A. S. (Editors), *Hypogene Cave Morphologies*: Karst Waters Institute, Leesburg, VA, pp. 4–12.

Klimchouk, A. B., 2018, Advances in understanding hypogene karst. In Stafford, K. W. and Veni, G. (Editors), *Hypogene Karst of Texas*: Monograph 3, Texas Speleological Survey, Austin, TX, pp. 3–15.

Levorsen, A. I., 1967, *Geology of Petroleum*: W. H. Freeman Co., New York, NY, 724 p.

Long, L. T. and Kaufmann, R. D., 2013, *Acquisition and Analysis of Terrestrial Gravity Data*: Cambridge University Press, Cambridge, U.K., 171 p.

Longman, M. W., 1982, Carbonate diagenesis as a control on stratigraphic traps. In *Proceedings of the 1981 AAPG Education Conference in Calgary, Canada*: American Association of Petroleum Geologist Department of Education, Course Note Series No. 21, Tulsa OK, 159 p.

Mathur, R.; Mutti, L.; Barra, F.; Gold, D.; Smith, R. C.; Doden, A.; Detrie, T.; Ruiz, J.; and McWilliams, A., 2008, Fluid inclusion and Re-Os isotopic evidence for hot Cenozoic mineralization in the central Pennsylvanian Valley and Ridge Province: *Mineralogy and Petrology*, Vol. 93, No. 3–4, pp. 309–324.

Mathur, R.; Gold, D. P.; Ellsworth, C. J.; Doden, A.; Wilson, M.; Ruiz, J.; Shcheetz, B. E.; and Herman, G. C., 2015, Re-Os isotope evidence of Early Tertiary crustal faulting and sulfide-mineralization in Pennsylvania with probable ties to the Chesapeake Bay bolide impact in Maryland, USA. In Herman, G. C. and Ferguson, S. M. (Editors), *Neotectonics of the New York Recess; Geological Association of New Jersey XXXII Annual Conference and Field Trip*: Geological Association of New Jersey, Trenton, NJ, pp. 68–79.

Miles, C. E. and Whitfield, T. G., compilers, 2001, *Bedrock Geology of Pennsylvania*, Edition 1.0 [digital map]: *Pennsylvania Bureau of Topographic and Geologic Survey, Department of Conservation and Natural Resources*, Harrisburg, PA, scale 1:250,000.

Milsom, J., 1989, *Field Geophysics*: Open University Press, New York, NY, 182 p.

Moritz, H., 1980, Geodetic Reference System 1980: *Journal of Geodesy*, Vol. 74, No. 1, pp. 128–133.

Nettleton, L. L., 1976, *Gravity and Magnetics in Oil Prospecting*: McGraw-Hill, New York, NY, 464 p.

Nick, K. E. and Elmore, R. D., 1990, Paleomagnetism of the Cambrian Royer Dolomite and Pennsylvanian Collings Ranch Conglomerate, southern Oklahoma: An early Paleozoic magnetization and nonpervasive remagnetization by weathering: *Geological Society of America Bulletin*, Vol. 102, No. 11, pp. 1517–1525.

Nickelsen, R. P., 1988, Structural evolution of folded thrusts and duplexes on a first-order anticlinorium in the Valley and Ridge Province of Pennsylvania. In Mitra, G. and Wojtal, S. (Editors), *Geometries and Mechanics of Thrusting with Special Reference to the Appalachians*: Special Paper 222, Geological Society of America, Boulder, CO, pp. 89–106.

Oliver, J., 1986, Fluids expelled tectonically from orogenic belts: Their role in hydrocarbon migration and other geologic phenomena: *Geology*, Vol. 14, No. 2, pp. 99–102.

Parizek, R. R.; White, W. B.; and Langmuir, D., 1971, *Hydrogeology and Geochemistry of Folded and Faulted Rocks of the Central Appalachian Type and Related Land Use Problems*: Circular 82, The Pennsylvania State University College of Earth and Mineral Sciences, University Park, PA, 210 p.

Rauch, H. W., and White, W. B., 1970, Lithologic controls on the development of solution porosity in carbonate aquifers: *Water Resources Research*, Vol. 6, No. 4, pp. 1175–1192.

Reynolds, J. M., 2011, *An Introduction to Applied and Environmental Geophysics*: Wiley-Blackwell, New York, NY, 796 p.

Sauro, U., 2012, Closed depressions in karst areas. In Culver, D. C. and White, W. B. (Editors), *Encyclopedia of Caves*: Academic Press, Amsterdam, pp. 140–155.

Sibley, D. F., 1982, The origin of common dolomite fabrics: Clues from the Pliocene: *Journal of Sedimentary Research*, Vol. 52, No. 4, pp. 1087–1100.

Stewart, M. T., 1980, Gravity survey of a deep buried valley: *Ground Water*, Vol. 18, No. 1, pp. 24–30.

Wilson, J. L., 1975, *Carbonate Facies in Geologic History*: Springer, Berlin, 472 p.

Woollard, G. P., 1975, Regional changes in gravity and their relation to crustal parameters. *Bureau Gravimetrique International Bulletin d'Information*, Vol. 36, pp. 106–110.